Special Issue Article

Advances in Mechanical Engineering

Advances in Mechanical Engineering
2015, Vol. 7(7) 1–17

DOI: 10.1177/1687814015593873
aime.sagepub.com
SAGE

Study on shear resistance of fiber-reinforced polymer–reinforced concrete beams

Juozas Valivonis, Marius Budvytis, Mantas Atutis, Edgaras Atutis and Linas Juknevičius

Abstract

This article is aimed to investigate the shear resistance of the beams reinforced with fiber-reinforced polymer stirrups. Together with theoretical analysis of the existing shear resistance provisions in design codes and literature, an experimental research was performed. During the experimental investigation, four doubly reinforced rectangular concrete beams were designed, produced, and tested to failure. A new analytical calculation method (including, but not limited to statistical validation) to investigate the shear response of fiber-reinforced polymer–reinforced concrete beams has been developed. A database with 102 beams was compiled, in order to evaluate the guideline provisions and proposed analytical calculation method. The experimental results were compared with theoretical results obtained by the proposed analytical calculation method. Correlation between analytical and experimental results is more accurate than using the existing provisions in design codes and literature for fiber-reinforced polymer–reinforced concrete beams.

Keywords

Fiber-reinforced polymer reinforcement, reinforced concrete structures, shear, resistance, statistical analysis

Date received: 6 November 2014; accepted: 17 April 2015

Academic Editor: Yu-Fei Wu

Introduction

Concrete structural members are usually reinforced with non-prestressed steel reinforcement or prestressed steel tendons. These structural members are sufficiently durable because high alkalinity of concrete protects steel reinforcement from corrosion. However, there are vast structures, such as water treatment facilities, chemical storage tank systems, concrete bridges, and dock and pier structures, which are exposed to aggressive environment and where these structures are affected by deicing salts, humidity, and temperature. The aggressive conditions reduce alkalinity of concrete. It leads to corrosion of steel reinforcement. Also it is not advisable to use steel reinforcement in structures that are exposed to electromagnetic fields. Because of the reasons listed above, fiber-reinforced polymer (FRP) reinforcement, which consists of fibers impregnated in a resin matrix, could be a good replacement for steel reinforcement. Non-magnetic properties of FRP reinforcement, corrosive resistance and high tensile strength, allow it to be used as reinforcement for concrete structural members.[1–6] Test results showed that non-metallic reinforcement can be used for structures such as reactor base mats, airport runway structures, and electronics laboratories or for the structures where medical equipment is stored.[7] Furthermore, often FRP materials are used for strengthening of concrete structures.[8–13]

Department of Reinforced Concrete and Masonry Structures, Vilnius Gediminas Technical University, Vilnius, Lithuania

Corresponding author:
Juozas Valivonis, Department of Reinforced Concrete and Masonry Structures, Vilnius Gediminas Technical University, Saulėtekio al. 11, LT-10223 Vilnius, Lithuania.
Email: juozas.valivonis@vgtu.lt

The application of FRP materials in civil engineering is recognized worldwide. Various organizations in countries such as United States,[14] Canada,[15] Great Britain,[16] Japan,[4] and Italy[17] released design guidelines, recommendations, and standards, where FRP reinforcement is considered as the main reinforcement in concrete structural members.

FRP reinforcement can be used as longitudinal and shear reinforcement. Shear reinforcement is used when concrete shear capacity is exceeded. Usually, shear reinforcement is used as closed stirrups. However, manufacturing of these closed stirrups is not simple. FRP reinforcement can be bent when resin is not hardened yet or by heating already cured resin. Stirrup can be formed by heating a straight FRP bar and bending it into the desired shape.[18] Lees'[19] experimental study of carbon, aramid, and glass fiber–reinforced polymer (GFRP) bars has shown that when ratio of bar's radius and diameter is 3, 5, and 7, tensile strength of the corner of the bent stirrup is approximately 45%, 55%, and 65% of the straight bar's tensile strength. However, it is noted that these results depend on the type of the fiber and resin, as well as on the method of forming the stirrup.[4] It was found that in order to achieve 50% of the straight bar's tensile strength in the corner of the bent stirrup, ratio of GFRP bar's radius and diameter has to be 4, while the ratio of carbon fiber–reinforced polymer (CFRP) bar's radius and diameter has to be 7.[20]

When separate straight FRP bars are used for shear reinforcement in concrete beams, anchorage of these straight FRP bars becomes an issue. Efficiency of anchorage directly depends on FRP bar's surface roughness. FRP bar's surface roughness depends on reinforcement's manufacturing method. Physical properties of FRP bar's surface determine the bond strength between reinforcement and concrete.

Comparing two beams reinforced with the same amount of reinforcement, one with steel reinforcement and another with FRP reinforcement, in latter beam, the depth of the compression zone after cracking is smaller due to smaller modulus of elasticity of FRP reinforcement.[21] Section's depth of the compression zone is smaller and crack widths are larger. Because of the reasons mentioned above and due to aggregate interlock, shear transfer in the compression zone and across cracks decreases. Regarding the results of experimental studies, where concrete beams without shear reinforcement were tested, it was stipulated that shear resistance depends on the area of longitudinal reinforcement and modulus of elasticity.

Current shear resistance design recommendations

Most of the available calculation models for shear resistance of concrete beams reinforced with FRP reinforcement are based on methods and assumptions, which are applied to evaluate the shear resistance for beams reinforced with steel. In addition to this, the current methods are based on a theory that shear capacity of reinforced concrete beam consists of concrete shear resistance V_c and FRP transverse reinforcement shear resistance V_f.[21–25] Likewise, one of the main assumptions of this theory introduces mechanisms, which transfer shear stresses, are plastic and redistribution of stresses can occur. However, FRP reinforcement is an elastic and brittle reinforcement, which is not characterized by plastic behavior. Consequently, the question is whether calculation models aimed for calculation of shear capacity for steel-reinforced elements can be used for the design of FRP-reinforced beams.[26]

The results of experimental investigations, carried out by various authors,[27–35] show that shear capacity of concrete beams reinforced with longitudinal and transverse FRP reinforcement can be verified with sufficient margin by applying classical methods, which are mainly used for the design of beams reinforced with conventional reinforcement. However, it is therefore highly recommended to limit the maximum strain in FRP shear reinforcement. This restriction is applied in separate design guidelines or recommendations as per American Concrete Institute (ACI) 440.1R-06 or Japan Society of Civil Engineers (JSCE).

First, the limit of maximum strain was set to 0.002–0.0025, by analogy to the yielding strain of steel. After more experiments were performed, it was suggested that the limit value could be higher. In order to use all advantages of FRP reinforcement, these higher values are used in many design recommendations currently.

ACI 440.1R-06 and JSCE design recommendations

According to ACI 440.1R-06 and JSCE design recommendations, the shear capacity of FRP-reinforced concrete beam can be estimated using the following equation

$$V_u = V_c + V_f \tag{1}$$

where V_c is the concrete shear resistance; V_f is the FRP transverse reinforcement shear resistance.

Concrete shear resistance, according to ACI 440.1R-06

$$V_c = \frac{2}{5}\sqrt{f_c}b_w c \tag{2}$$

$$c = kd \tag{3}$$

$$k = \sqrt{2\rho_f n_f + (\rho_f n_f)^2} - \rho_f n_f \tag{4}$$

where c is the depth of compression zone at cracked transformed section; k is the coefficient, which accounts the decreasing depth of neutral axis.

Concrete shear capacity according to JSCE could be calculated as follows

$$V_c = \beta_d \beta_p \beta_n f_{vc} b_w d \tag{5}$$

$$\beta_d = \sqrt[4]{\frac{1}{d}} \leq 1.5 \tag{6}$$

$$\beta_p = \sqrt[3]{100\rho_f E_f / E_s} \leq 1.5 \tag{7}$$

$$f_{vc} = 0.2\sqrt[3]{f_c} \leq 0.72\,\mathrm{N/mm^2} \tag{8}$$

where β_d is the coefficient, by which the size effect is estimated; β_p is the coefficient, which accounts the specific properties of FRP reinforcement.

Shear capacity provided by FRP shear reinforcement, according to ACI 440.1R-06, can be calculated using the following equation

$$V_f = \frac{f_{fw} A_{fw} d}{s} \tag{9}$$

where f_{fw} is the stress level in the FRP shear reinforcement at the ultimate state.

The stress level in the FRP stirrups f_{fw} is limited, in order to limit shear crack width and to avoid rupture of FRP stirrup in the bent portion of the bar

$$f_{fw} = 0.004 E_{fw} \leq f_{fb} \tag{10}$$

$$f_{fb} = \left(0.05 \cdot \frac{r_b}{d_b} + 0.3\right) f_{fuw} \tag{11}$$

where f_{fb} is the tensile strength of FRP bent bar; r_b is the bending radius of FRP bar; d_b is the diameter of the FRP bar in the bent portion; f_{fuw} is the tensile strength of FRP shear reinforcement.

JSCE recommends calculating shear resistance of FRP shear reinforcement using this equation

$$V_f = \frac{A_{fw} E_{fw} \varepsilon_{fw}}{s} z \tag{12}$$

$$\varepsilon_{fw} = \sqrt{\left(\frac{h}{0.3}\right)^{-0,1} f_c \frac{\rho_f E_f}{\rho_{fw} E_{fw}}} \cdot 10^{-4} \tag{13}$$

$$z = \frac{d}{1.15} \tag{14}$$

where ε_{fw} is the strain in the FRP stirrup at the ultimate state; z is the lever arm of internal forces.

According to JSCE design recommendations, the stress level in the FRP stirrups is also limited

$$E_{fw} \varepsilon_{fw} \leq f_{fb} \tag{15}$$

where ε_{fw} is calculated according to equation (13) and f_{fb} is calculated according to equation (11).

Eurocode 2 design recommendations

This method originally was developed for evaluation of shear capacity for steel-reinforced concrete beams.[36] The Eurocode 2 (EC 2) proposes method that is based on a truss model.

According to EC 2, shear resistance for concrete beams reinforced with transverse reinforcement

$$V_u = \min \begin{cases} V_{u,f} = \frac{A_{fw}}{s} z f_{fw} ctg\theta \\ V_{u,\max} = \alpha_{cw} b_w z \nu_1 f_c / (ctg\theta + tg\theta) \end{cases} \tag{16}$$

$$z = 0.9d \tag{17}$$

$$\nu_1 = 0.6\left[1 - \left(\frac{f_c}{250}\right)\right] \tag{18}$$

$$ctg\theta = \sqrt{\frac{\alpha_{cw} b_w \nu_1 f_c s}{A_{fw} f_{fw}} - 1} \tag{19}$$

where $V_{u,f}$ is the value of the shear force which can be resisted by the shear reinforcement; $V_{u,\max}$ is the value of the maximum shear force which can be sustained by the member, limited by crushing of the compression struts; θ is the angle between the concrete compression strut and the beam axis perpendicular to the shear force; α_{cw} is the coefficient taking into account the state of the stress in the compression chord; ν_1 is the strength reduction factor for concrete cracked in shear.

The recommended limiting values for $ctg\theta$

$$1 \leq ctg\theta \leq 2.5 \tag{20}$$

This restriction means that the angle between the concrete compression strut and the beam axis cannot be less than 21.8° and more than 45°.

Sato et al. shear resisting model. This shear resisting model was developed by the numerical study using nonlinear finite element program.[37] It is assumed that shear capacity of the cracked section can be evaluated using this equation

$$V_u = V_c + V_f + V_{str} \tag{21}$$

where V_{str} is the shear resisting force by other than transverse reinforcement at the shear cracking zone.

Furthermore, it was found that the largest shear capacity of the beam is at the section where its neutral axis intersects with the straight line, which connects the loading and supporting points. It is assumed in this model that the examined section consists of concrete compression zone at the loading point, shear crack zone, where section's shear resistance is the largest and horizontal zone, which connects compression and shear cracking zones (Figure 1). These assumptions can be written as

$$V_u = V_c + V_f + V_{str} - V_{com} \tag{22}$$

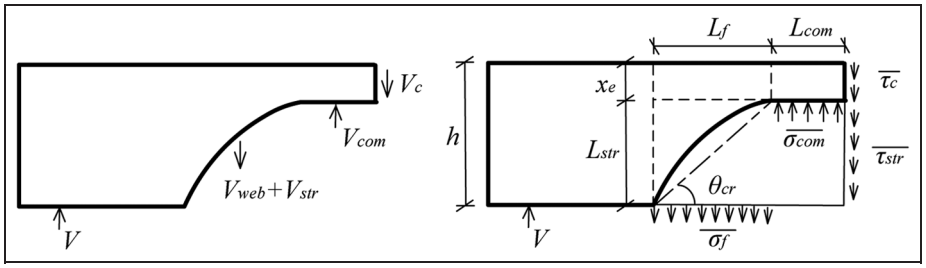

Figure 1. Shear resisting model and distribution of shear resisting stresses.

$$V_u = b_w x_e \bar{\tau}_c + \rho_{fw} b_w L_f \bar{\sigma}_f + b_w L_{str} \bar{\tau}_{str} - b_w L_{com} \bar{\sigma}_{com} \tag{23}$$

$$\bar{\tau}_c = 0.65 f_c \sin\alpha \cos\alpha \tag{24}$$

$$\bar{\sigma}_f = \bar{\varepsilon}_f E_{fw} \tag{25}$$

$$\bar{\varepsilon}_f = 0.0053 \frac{\sqrt{f_c}}{\sqrt{a/d}+1} e^{\left(-\frac{1000}{\rho_s E_s} - 0.05\sqrt{\rho_{fw} E_{fw}}\right)} \tag{26}$$

$$\bar{\tau}_{str} = f_c^{1/3} \frac{1.28}{\sqrt{a/d}+1} \tag{27}$$

$$\bar{\sigma}_{com} = 0.64 f_c \left(\frac{a}{d}\right)^{-1} \sin^2\beta \tag{28}$$

where V_{com} is the shear resisting force by concrete at the horizontal zone, which connects compression and shear cracking zones; α is the angle of the principal stress at the compression zone; β is the angle of the principal stress at the horizontal zone.

Proposed shear design model

Proposed shear design model is also based on the assumption that shear strength consists of concrete shear capacity as well as FRP transverse reinforcement shear capacity. However, these two components can be evaluated differently from previously reviewed design provisions.

In the proposed model, shear resistance is calculated according to equation (1).

It is known that the resultant shear force of shear stresses caused at cross section can be calculated

$$V_c = \bar{\tau}_c b_w x_e \tag{29}$$

where $\bar{\tau}_c$ is the average shear stresses at the compression zone, and x_e is the depth of the compression zone.

It is known that the limiting values of average shear stresses are approximately equal to

$$\bar{\tau}_c \approx 2 f_{ct} \tag{30}$$

It is also known that shear cracking angle for reinforced concrete beam may vary from 26° to 45°. Assuming that shear cracking angle is equal to 45° and taking into account equation (29), concrete shear resistance can be calculated

$$V_c = \varphi_{c2} f_{ct} b_w d \tag{31}$$

Reinforced concrete experimental studies have shown that when shear cracking angle is less than 45°, concrete shear resistance decreases. The influence of shear cracking angle on concrete shear resistance V_c can be evaluated using ratio of shear span a and effective depth d. In that case, concrete shear resistance of concrete beams without shear reinforcement can be calculated

$$V_c = \frac{\varphi_{c2} f_{ct} b_w d}{a/d} = \frac{\varphi_{c2} f_{ct} b_w d^2}{a} \tag{32}$$

The influence of FRP flexural reinforcement for the concrete shear resistance V_c is evaluated using coefficient φ_f. Therefore, the following equation is proposed for calculating concrete shear capacity of concrete beams reinforced with FRP flexural reinforcement

$$V_c = \frac{\varphi_{c2} \varphi_f f_{ct} b_w d^2}{a} \geq \varphi_{c3} \varphi_f f_{ct} b_w d \tag{33}$$

Coefficient φ_f, which estimates the specific flexural FRP reinforcement's properties, is determined by analyzing the results of experimental tests, which are given in section "Review of the existing experimental tests"

$$\varphi_f = 0.4 \cdot \left(\frac{E_{flex.}}{E_s}\right)^{\rho_{flex.}} \tag{34}$$

where $E_{flex.}$ is the modulus of elasticity of flexural reinforcement; $\rho_{flex.}$ is the flexural reinforcement ratio.

Research shows that when shear span a increases, concrete shear resistance V_c decreases significantly. In the case of high shear span a values, experimental concrete shear resistance significantly differs from the calculated strength. Taking that into account, the maximum value of shear span a is limited

$$a \leq \frac{\varphi_{c4}}{\varphi_{c3}} d \tag{35}$$

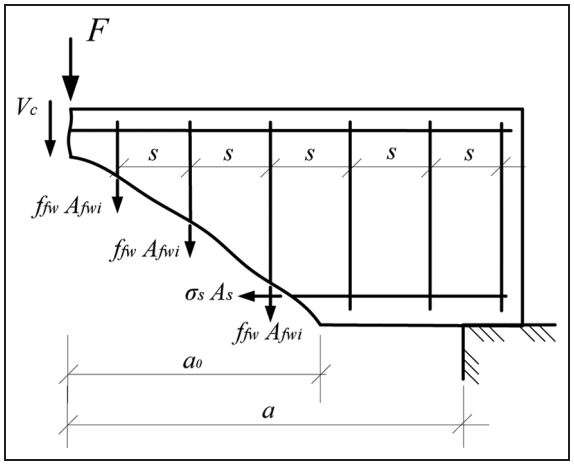

Figure 2. Shear resisting model.

Coefficients φ_{c2}, φ_{c3}, and φ_{c4}, which estimate concrete's properties, are proposed as follows:

- For normal weight concrete

$$\varphi_{c2} = 2.0;\ \varphi_{c3} = 0.45;\ \varphi_{c4} = 1.5$$

FRP transverse reinforcement shear capacity V_f is determined by summing up multiplied values of FRP shear reinforcement area A_{fw} and tensile strength f_{fw}

$$V_f = \sum_{i=1}^{n} f_{fw} A_{fwi} \tag{36}$$

where A_{fwi} is the area of one FRP reinforcement bar; n is the number of transverse reinforcement bars in the shear cracking zone.

Critical projection of shear cracking zone, where FRP shear reinforcement contributes to shear strength of concrete beam, is indicated as a_0 (Figure 2).

Shear strength caused by web reinforcement in the structural member's linear meter

$$\nu_{fw} = \frac{f_{fw} A_{fw}}{s} \tag{37}$$

FRP transverse reinforcement shear capacity can be expressed by the following equation

$$V_f = \sum_{i=1}^{n} f_{fw} A_{fwi} = \nu_{fw} a_0 \tag{38}$$

In order to calculate critical projection a_0, the following assumptions are accepted

$$V_c = V_f, a = a_0 \tag{39}$$

Therefore, the following expression can be written

$$\frac{\varphi_{c2}\varphi_f f_{ct} b_w d^2}{a_0} = \nu_{fw} a_0 \tag{40}$$

From equation (40), critical projection a_0

$$a_0 = \sqrt{\frac{\varphi_{c2} f_{ct} b_w d^2}{\nu_{fw}}} \tag{41}$$

As previously mentioned, shear cracking angle may vary from 26° to 45°. Also, critical projection a_0 always has to be smaller than shear span a, because web reinforcement does not transfer shear stresses uniformly along beam's axis. Because of these reasons, critical projection a_0 is limited

$$d \le a_0 = \sqrt{\frac{\varphi_{c2} f_{ct} b_w d^2}{\nu_{fw}}} \le \min \begin{cases} 2d \\ a \end{cases} \tag{42}$$

The stress level in the FRP stirrups f_{fw} is determined by the following equation

$$f_{fw} = \varepsilon_{fw,\,\mathrm{lim}} \cdot E_{fw} \tag{43}$$

The maximum strain in the FRP stirrup is determined by analyzing experimental data, which were compiled from tests performed by the authors of this article and other researchers. The maximum strain is suggested as follows:

- For beams reinforced with flexural steel reinforcement and shear FRP reinforcement

$$\varepsilon_{fw} = \sqrt{\left(\frac{h}{0.4}\right)^{-1.5} f_c \frac{\rho_{flex.} E_{flex.}}{\rho_{fw} E_{fw}}} \cdot 10^{-4} \le 0.0045 \tag{44}$$

- For beams reinforced with both flexural and shear FRP reinforcement

$$\varepsilon_{fw} = \sqrt{\left(\frac{h}{0.85}\right)^{-1,5} f_c \frac{\rho_{flex.} E_{flex.}}{\rho_{fw} E_{fw}}} \cdot 10^{-4} \le 0.0045 \tag{45}$$

The maximum strain in the FRP stirrups is limited in order to control shear crack width.

Experimental study

Experimental study by authors

Materials and specimens. In this study, experimental tests of concrete beams, reinforced with flexural steel reinforcement and straight GFRP bars as shear reinforcement, were carried out. The mechanical properties of concrete and GFRP reinforcement were determined experimentally. The compressive strength, tensile strength, and modulus of elasticity of the concrete were evaluated by

Figure 3. Testing of the GFRP reinforcement bar.

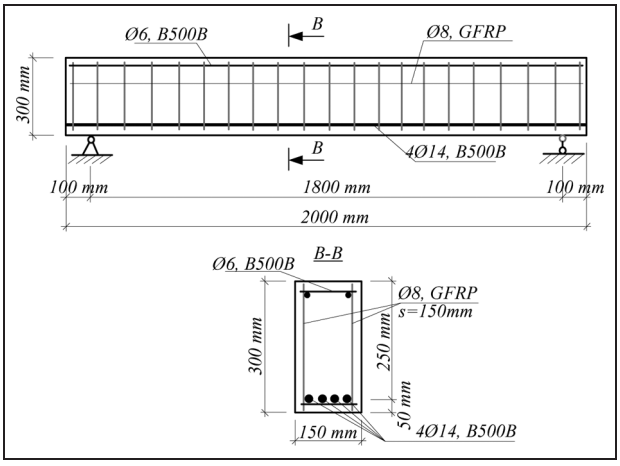

Figure 4. Details of test beams.

testing standard cubes, standard cylinders, and standard prisms, which were cast at the same time and cured under the same conditions as the test specimens. Dimensions of standard cubes were 150 × 150 × 150 mm, standard cylinders 150 × 300 mm, standard prisms 100 × 100 × 400 mm. Six cubes and three cylinders were tested according to the requirements of EN 12390-3:2009. The mean value obtained for the cube compressive strength was 36.3 N/mm^2. The mean cylinder compressive strength and modulus of elasticity were determined from the results of cylinder testing. The mean cylinder compressive strength was 29.0 N/mm^2. The mean value obtained for the modulus of elasticity was 26.5×10^3 N/mm^2. The mean tensile strength was determined by testing prisms according to the requirements of EN 12390-5:2003. The mean value obtained for the tensile strength was 3.34 N/mm^2.

The characteristic yield strength of the steel bars used to reinforce beams was 500 N/mm^2. The GFRP bars used to reinforce beams in shear were produced by *Schock ComBAR*. The mechanical properties of GFRP bars were determined by direct tension test (Figure 3). Bars were tested according to the requirements of ISO 10406-1. Four GFRP bars were tested. The mean value obtained for the tensile strength of GFRP bar was 1418.2 N/mm^2, the mean value obtained for the elastic modulus was 6.2×10^3 N/mm^2, and the ultimate strain was 2.36%.

Four doubly reinforced rectangular concrete beams were constructed for experimental testing. Beams were reinforced with four 14-mm-diameter steel bars (A_s = 616 mm^2) in the tension zone and with two 6-mm diameter steel bars (A_s = 57 mm^2) in the compression zone of the beam.

The carried out tests[38,39] showed that tensile strength of FRP bar was significantly reduced because of tensile and shear stresses acting together. The test results showed that failure of the FRP stirrups occurs in the corner of the bent stirrup. Because of the aforesaid, through experimental program, the objective was to investigate the influence of straight FRP bars, used as shear reinforcement, for shear strength of the specimens. Therefore, specimens of this experimental study were reinforced with straight FRP shear reinforcement bars. The beams were reinforced with 8-mm-diameter GFRP bars, and the spacing of the bars was 150 mm. The details of the test beams are illustrated in Figure 4. The cages of reinforcement in the formwork of the beams are shown in Figure 5.

Experimental setup and instrumentation. In this experimental study, reinforced concrete beams were subjected to three-point bending. The loading point was 350 mm away from support (Figure 6). Strains were measured by inductive sensors attached on the surface of the specimens. The layout of inductive sensors is shown in Figure 6. Concrete strains were measured by the inductive sensors in the compression and tension zones of the specimens, as well as in the shear cracking zone. Crack widths were monitored by optical microscope with an accuracy of 0.05 mm. During the test, load was applied in increments of 10 kN. After every increment, crack widths were measured. Crack widths were

Figure 5. Reinforcement cages in the formwork of the beams.

measured until applied load was about 60% of estimated theoretical shear strength of the specimen.

Test results. The specimens of this experimental study (S-3-A, S-4-A, S-3-B, S-4-B) were subjected to one concentrated load (Figure 6). During experimental work, the objective was to obtain shear strength, strains in the concrete, and failure mode for all concrete beams. The shear failure was observed for all tested beams. The failure and crack opening modes (Figure 7) were very similar for all specimens, because of same geometrical properties as well as the amount of reinforcement.

The experimental shear strength for beam S-3-B was $V_{exp} = 202.9\,\text{kN}$, for S-4-B was $V_{exp} = 223.9\,\text{kN}$, for S-3-A was $V_{exp} = 191.5\,\text{kN}$, and for beam S-4-A was $V_{exp} = 182.5\,\text{kN}$. The test results show that out of four reviewed calculation models, only shear strength values obtained by Sato et al. and JSCE methods are smaller than the experimental results ($V_{calc,Sato} = 134.2\,\text{kN}$, $V_{calc,JSCE} = 59.5\,\text{kN}$). The shear strength values obtained by EC 2 and ACI 440.1R-06 equations were larger than the experimental shear strength values ($V_{calc,EC} = 271.3\,\text{kN}$, $V_{calc,ACI} = 270.7\,\text{kN}$). Tensile strength of the GFRP shear reinforcement bars was not limited using EC 2 and ACI 440.1R-06 calculation methods. Straight GFRP bars were used as shear reinforcement; therefore, tensile strength did not decrease because of bending of the bar. Tensile stress level in the shear reinforcement depends on the calculated strain, when calculations are made using Sato et al. and JSCE design recommendations. Due to lower tensile strength of the bar, the calculated theoretical shear strength was lower than experimental.

During the testing in all the tested beams, the vertical crack in the tension zone of the beam under the loading point opened first. First, vertical crack opened up in beam S-3-A, when applied load was $F = 39.5\,\text{kN}$ (stress in the tensile concrete zone was $\sigma_{ct} = 4.95\,\text{N/mm}^2$), in beam S-4-A was $F = 50.0\,\text{kN}$ ($\sigma_{ct} = 6.27\,\text{N/mm}^2$), in S-3-B was $F = 40.0\,\text{kN}$ ($\sigma_{ct} = 4.55\,\text{N/mm}^2$), and in S-4-B was $F = 50.0\,\text{kN}$ ($\sigma_{ct} = 5.69\,\text{N/mm}^2$). In all these cases, concrete stresses in the tension zone of the beam exceeded the mean concrete tensile strength value ($f_{ctm} = 3.34\,\text{N/mm}^2$), when first vertical crack opened up. Load–strain (measured by T_4 inductive sensor) responses for tested beams are shown in Figure 8. It can be seen from this graph how concrete strains change after opening of the first vertical crack. The first vertical crack is shown in Figure 7. The width of this

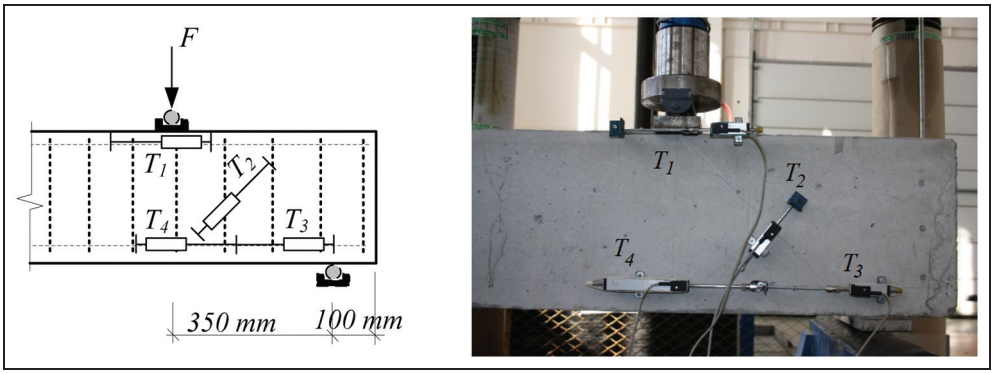

Figure 6. Test arrangement.

Figure 7. Cracking pattern at failure for the test specimens

crack gradually increased until applied load was about 30% of the calculated shear strength.

The first shear cracks formed when applied load was increased. At the same time, the first shear crack in beam S-3-A formed, when applied load was 27.8% of the calculated shear strength ($F = 66.1$ kN), in beam S-4-A 34.6% ($F = 78.3$ kN), S-3-B 27.9% ($F = 77.4$ kN), and S-4-B 23.9% ($F = 73.1$ kN). In general, shear cracks formed when maximum tensile stresses, which depend on specimen's geometrical properties and applied loads, were developed. It should be said that mechanical properties of shear reinforcement do not influence the quantity of these stresses. The obtained results were very similar because of the same properties of the specimens.

When first shear crack was formed, the value of the load was determined based on load–strain (measured by T_2 inductive sensor) relationships shown in Figure 9. In order to determine the moment of the shear crack formation as accurately as possible and its further development, concrete strains regarding shear cracking zone were measured by inductive sensor T_2.

It can be seen from this graph that concrete strains increase linearly with increasing load until first shear crack forms. After the formation of first shear cracks, concrete strains increase nonlinearly. Moreover, shear cracks develop in the direction of maximum compressive stresses, and this direction changes in each case—that is why graphs in Figure 9 are different. Furthermore, after formation of shear cracks, GFRP shear reinforcement restrains the growth of shear cracks. Therefore, concrete strains are also related to quality of anchorage of shear reinforcement.

Review of the existing experimental tests

From reliability point of view, to verify proposed shear design model and to compare current available calculation models, test results of 102 concrete beams, reinforced with FRP shear reinforcement, were collected. The analysis showed that beams, reinforced with FRP shear reinforcement, can be reinforced with flexural steel or non-metallic reinforcement.

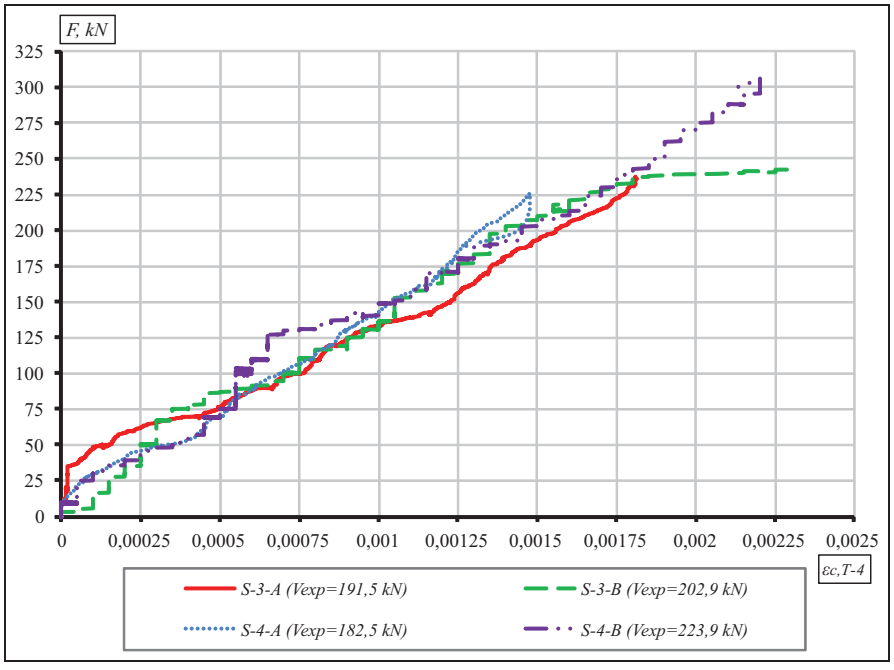

Figure 8. Load–strain (measured by T_4 inductive sensor) relationships of tested beams.

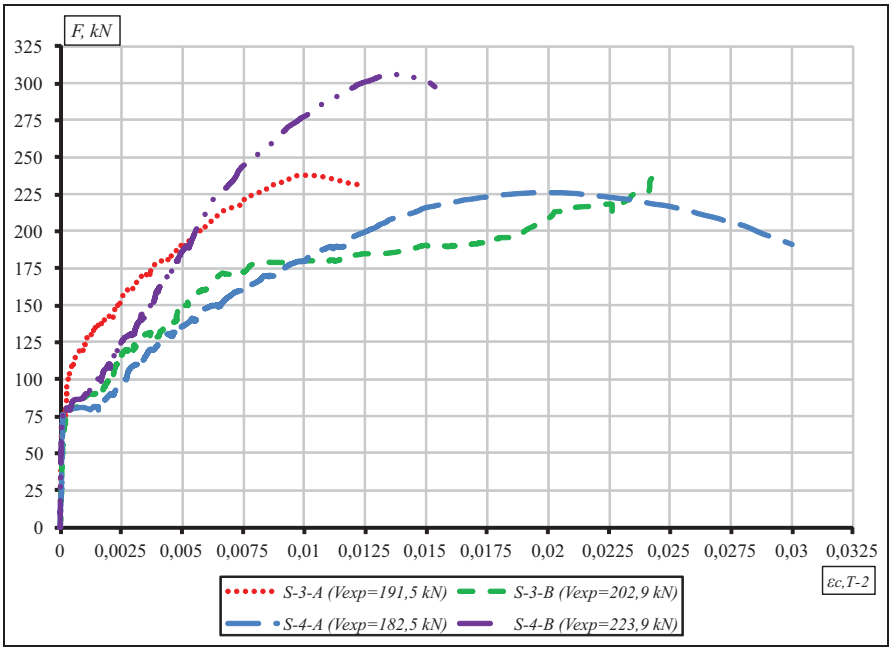

Figure 9. Load–strain (measured by T_2 inductive sensor) relationships of tested beams.

The collected database included 27 beams, reinforced with flexural steel reinforcement and FRP shear reinforcement (Table 1).[40–44] This database consists of concrete beams with different geometrical properties, concrete mechanical properties, and different types and amounts of reinforcement.

The collected database also included 75 beams, reinforced with both flexural and shear FRP reinforcement.[20,27,43–48] The details of the beams are shown in Table 2.

Verification of the proposed shear design model

In order to verify the proposed shear design model, comparison of experimental and theoretical shear strength values, calculated using reviewed and proposed calculation methods, was performed. The four specimens, tested by the authors of this article, were also included in the analysis. The results of this analysis are shown in Figures 10–12 and are discussed further in this article.

It can be seen from Figure 12 that for the proposed shear design model, the average value of V_{exp}/V_{calc} is 1.02 with standard deviation of 0.25 and coefficient of variation of 24.2%. According to these results, systematic error is 0.02 and random error is equal to 0.25 for the proposed calculation method for beams, reinforced with FRP shear reinforcement.

It should be noted that the compiled database included specimens with very different geometrical characteristics (width of the web varies from 135 to 450 mm, effective depth varies from 250 to 600 mm), reinforced with different types of FRP reinforcement (aramid fiber–reinforced polymer reinforcement (AFRP), GFRP, CFRP, vinyl fiber–reinforced polymer reinforcement (VFRP)) and steel reinforcement, and with different amounts of reinforcement (longitudinal reinforcement ratio varies from 0.53% to 4.65%, transverse reinforcement ratio varies from 0.04% to 1.50%). All these variables influence standard deviation and coefficient of variation of the proposed model.

It can be seen from Figures 10 and 12 that the biggest difference between theoretical calculations and experimental results of shear strength is for specimens, tested by the authors. As already discussed above, straight GFRP bars were used as shear reinforcement in the experimental study, performed by the authors, while other specimens were reinforced with FRP stirrups. In order to draw conclusions about the calculation of shear resistance for beams reinforced with straight FRP bars, more experimental studies have to be performed.

Theoretical shear resistance was calculated for all specimens from the compiled database (Tables 1 and 2), using ACI 440.1R-06, JSCE, EC 2, and Sato et al. design recommendations also. The performed analysis of the current available design guidelines, recommendations, and shear strength of beams reinforced with FRP reinforcement has shown that there is no universal calculation method to correctly evaluate maximum strain in the FRP shear reinforcement, which may affect the shear strength of concrete beams. The maximum strain

Table 1. Details of beams, reinforced with flexural steel reinforcement and FRP shear reinforcement.

Author	Specimen no.	Geometrical properties				f_c (N/mm^2)	Flexural reinforcement		Shear reinforcement				V_{exp} (kN)
		b_w (mm)	h (mm)	d (mm)	a/d		ρ_s (%)	$E_s \times 10^3$ (N/mm^2)	Type	ρ_{fw} (%)	f_{fu} (N/mm^2)	$E_{fw} \times 10^3$ (N/mm^2)	
Ahmed et al.[40]	1	180	700	600	3.30	42.2	1.17	200	CFRP	0.26	1538	130	376.0
	2	180	700	600	3.30	35.0	1.17	200	CFRP	0.39	1538	130	440.0
	3	180	700	600	3.30	35.8	1.17	200	CFRP	0.53	1538	130	536.0
Shehata[41]	4	135	560	470	3.72	54.0	1.32	200	CFRP	0.24	1800	137	277.5
	5	135	560	470	3.72	54.0	1.32	200	CFRP	0.36	1800	137	341.0
	6	135	560	470	3.72	51.0	1.32	200	CFRP	0.47	1800	137	375.5
	7	135	560	470	3.72	54.0	1.32	200	GFRP	0.71	713	41	292.0
	8	135	560	470	3.72	33.0	1.32	200	GFRP	1.05	713	41	312.0
	9	135	560	470	372	33.0	1.32	200	GFRP	1.40	713	41	311.5
Alsayed et al.[42]	10	200	360	310	2.36	35.7	0.99	200	GFRP	0.40	565	42	144.4
Nakamura and Higai[43]	11	200	300	250	3.00	34.7	1.72	180	GFRP	0.23	544	31	96.4
	12	200	300	250	3.00	34.4	1.72	180	GFRP	0.23	649	31	106.3
	13	200	300	250	3.00	35.6	1.72	180	GFRP	0.14	544	31	79.8
	14	200	300	250	3.00	35.8	1.72	180	GFRP	0.14	649	31	79.8
Tottori and Wakui[44]	15	200	330	285	2.11	37.2	4.07	206	VFRP	0.54	602	36	230.5
	16	200	330	285	2.11	37.2	4.07	206	VFRP	0.27	602	36	221.7
	17	200	330	285	3.16	35.3	4.07	206	VFRP	0.54	602	36	169.7
	18	200	330	285	3.16	35.3	4.07	206	VFRP	0.27	602	36	137.3
	19	200	330	285	3.16	35.3	4.07	206	VFRP	0.18	602	36	117.7
	20	200	330	285	4.21	31.4	4.07	206	VFRP	0.27	602	36	115.8
	21	200	400	325	3.23	42.2	0.86	192	VFRP	0.41	602	36	157.9
	22	200	400	325	3.23	71.6	0.86	192	VFRP	0.41	602	36	165.8
	23	200	400	325	4.31	50.6	0.86	192	VFRP	0.41	602	36	150.1
	24	200	400	325	4.31	65.7	0.86	192	VFRP	0.41	602	36	153.0
	25	150	300	250	2.50	29.4	2.06	206	CFRP	0.12	1283	94	105.9
	26	150	300	260	3.08	38.8	2.98	206	AFRP	0.13	1766	53	84.9
	27	200	300	250	3.20	40.7	4.65	206	AFRP	0.38	1278	64	191.8

CFRP: carbon fiber–reinforced polymer; GFRP: glass fiber–reinforced polymer; VFRP: vinyl fiber–reinforced polymer reinforcement; AFRP: aramid fiber–reinforced polymer reinforcement.

Table 2. Details of beams, reinforced with flexural FRP reinforcement and FRP shear reinforcement.

Author	Specimen no.	Geometrical properties			f_c (N/mm^2)	Flexural reinforcement			Shear reinforcement			V_{exp} (kN)
		b_w (mm)	d (mm)	a/d		Type	ρ_f (%)	$E_f \times 10^3$ (N/mm^2)	Type	ρ_{fw} (%)	$E_{fw} \times 10^3$ (N/mm^2)	
Tottori and Wakui[44]	1	200	325	3.2	44.4	CFRP	0.70	137	GFRP	0.15	40	103
	2	200	325	3.2	44.7	CFRP	0.70	137	GFRP	0.15	40	106
	3	200	325	3.2	44.9	CFRP	0.70	137	AFRP	0.07	69	85
	4	200	325	2.2	44.6	CFRP	0.70	137	CFRP	0.07	110	162
	5	200	325	3.2	44.8	CFRP	0.70	137	CFRP	0.07	110	83
	6	200	325	4.3	44.6	CFRP	0.70	137	CFRP	0.07	110	74
	7	200	325	3.2	45.0	CFRP	0.70	137	CFRP	0.04	144	98
	8	200	325	3.2	44.7	CFRP	0.70	140	CFRP	0.06	137	108
	9	200	325	3.2	44.7	CFRP	0.70	140	CFRP	0.10	137	157
	10	200	325	3.2	39.4	CFRP	0.70	140	AFRP	0.12	58	103
	11	200	325	3.2	39.4	AFRP	0.92	58	AFRP	0.09	58	83
	12	200	325	3.2	39.4	AFRP	0.92	58	AFRP	0.13	58	98
	13	200	325	3.2	39.4	AFRP	0.92	58	AFRP	0.23	58	132
	14	200	325	3.2	39.4	AFRP	0.92	58	AFRP	0.12	58	107
	15	200	325	3.2	39.4	AFRP	0.92	58	AFRP	0.12	58	78
	16	200	325	3.2	39.4	AFRP	0.92	58	CFRP	0.04	137	86
	17	150	250	2.5	35.5	CFRP	0.55	94	CFRP	0.12	94	58
	18	150	250	2.5	37.6	CFRP	0.55	94	CFRP	0.24	94	82
	19	150	250	2.5	34.3	CFRP	1.05	94	CFRP	0.12	94	71
	20	150	250	2.5	34.2	CFRP	2.11	94	CFRP	0.12	94	81
	21	300	500	2.5	31.9	CFRP	0.53	94	CFRP	0.06	94	160
	22	150	260	3.1	42.2	AFRP	3.08	63	AFRP	0.13	53	60
Nagasaka et al.[45]	23	250	253	1.2	29.5	AFRP	1.90	56	CFRP	0.50	115	251
	24	250	253	1.2	34.7	AFRP	1.90	56	CFRP	1.00	115	317
	25	250	253	1.2	33.5	AFRP	1.90	56	CFRP	1.50	115	366
	26	250	253	1.8	29.5	AFRP	1.90	56	CFRP	0.50	115	208
	27	250	253	1.8	29.5	AFRP	1.90	56	CFRP	1.00	115	282
	28	250	253	1.8	29.5	AFRP	1.90	56	CFRP	1.50	115	288
	29	250	253	2.4	33.5	AFRP	1.90	56	CFRP	0.50	115	162
	30	250	253	2.4	33.5	AFRP	1.90	56	CFRP	1.00	115	234
	31	250	253	1.8	34.1	AFRP	1.90	56	AFRP	0.50	62	205
	32	250	253	1.8	35.4	AFRP	1.90	56	AFRP	1.00	62	277
	33	250	253	1.8	35.4	AFRP	1.90	56	GFRP	0.50	47	179
	34	250	253	1.8	36.7	AFRP	1.90	56	GFRP	1.00	47	233
	35	250	253	1.8	24.0	AFRP	1.90	56	CFRP	1.00	115	211
	36	250	253	1.8	23.0	AFRP	1.90	56	CFRP	1.50	115	226
	37	250	253	2.4	24.8	AFRP	1.90	56	CFRP	1.00	115	186
	38	250	253	2.4	23.4	AFRP	1.90	56	CFRP	1.50	115	195
	39	250	253	1.8	23.0	AFRP	1.90	56	AFRP	1.00	62	194
	40	250	253	1.8	23.0	AFRP	1.90	56	AFRP	1.50	62	207
	41	250	253	1.8	40.3	AFRP	1.90	56	CFRP	1.50	115	298
	42	250	253	2.4	40.0	AFRP	1.90	56	CFRP	1.50	115	231

(continued)

Table 2. (continued)

Author	Specimen no.	Geometrical properties			f_c (N/mm^2)	Flexural reinforcement			Shear reinforcement			V_{exp} (kN)
		b_w (mm)	d (mm)	a/d		Type	ρ_f (%)	$E_f \times 10^3$ (N/mm^2)	Type	ρ_{fw} (%)	$E_{fw} \times 10^3$ (N/mm^2)	
Vijay and Kumar[46]	43	150	265	1.9	44.8	AFRP	1.43	54	AFRP	0.93	54	127
	44	150	265	1.9	44.8	AFRP	1.43	54	AFRP	0.62	54	115
	45	150	265	1.9	31.0	AFRP	0.64	54	AFRP	0.93	54	123
	46	150	265	1.9	31.0	AFRP	0.64	54	AFRP	0.62	54	123
Maruyama and Zhao[27]	47	150	250	2.5	36.2	CFRP	0.55	94	CFRP	0.12	94	59
	48	150	250	2.5	38.3	CFRP	0.55	94	CFRP	0.24	94	84
	49	150	250	2.5	35.0	CFRP	1.05	94	CFRP	0.12	94	73
	50	150	250	2.5	33.1	CFRP	1.10	94	CFRP	0.24	94	89
	51	150	250	2.5	31.3	CFRP	1.39	94	CFRP	0.24	94	95
	52	150	250	2.5	30.5	CFRP	2.11	94	CFRP	0.24	94	120
	53	150	250	2.5	30.5	CFRP	2.11	94	CFRP	0.18	94	86
	54	150	250	2.5	31.3	CFRP	2.11	94	CFRP	0.15	94	75
	55	150	250	2.5	34.9	CFRP	2.11	94	CFRP	0.12	94	83
Nakamura and Higai[43]	56	200	250	3.0	35.4	GFRP	1.61	29	GFRP	0.35	31	83
	57	200	250	3.0	33.4	GFRP	1.61	29	GFRP	0.35	31	100
	58	200	250	3.0	35.2	GFRP	1.61	29	GFRP	0.18	31	56
	59	200	250	3.0	35.2	GFRP	1.61	29	GFRP	0.18	31	66
Zhao et al.[47]	60	150	250	3.0	34.3	CFRP	3.02	105	GFRP	0.42	39	113
	61	150	250	3.0	34.3	CFRP	3.02	105	CFRP	0.42	100	126
	62	150	250	3.0	34.3	CFRP	2.27	105	GFRP	0.42	39	116
	63	150	250	2.0	34.3	CFRP	1.51	105	GFRP	0.42	39	123
	64	150	250	4.0	34.3	CFRP	1.51	105	GFRP	0.42	39	73
Maruyama and Zhao[28]	65	150	250	2.5	34.0	CFRP	1.07	100	GFRP	0.43	30	110
	66	150	250	2.5	34.0	CFRP	1.07	100	GFRP	0.43	30	107
	67	150	250	2.5	34.0	CFRP	1.07	100	GFRP	0.43	30	148
	68	150	250	2.5	34.0	CFRP	1.07	100	GFRP	0.43	30	131
	69	300	500	2.5	29.5	CFRP	1.07	100	GFRP	0.86	30	370
Alsayed et al.[42]	70	200	310	3.2	29.5	GFRP	1.37	36	GFRP	0.21	42	69
	71	200	309	2.4	29.6	GFRP	1.28	43	GFRP	0.40	42	109
Duranovic et al.[48]	72	150	230	3.3	33.0	GFRP	1.31	45	GFRP	0.35	45	49
	73	150	230	2.2	33.0	GFRP	1.31	45	GFRP	0.35	45	67
Shehata et al.[20]	74	135	470	3.2	50.0	CFRP	1.25	137	CFRP	0.29	137	305
	75	135	470	3.2	50.0	CFRP	1.25	137	GFRP	1.07	41	305

CFRP: carbon fiber–reinforced polymer; AFRP: aramid fiber–reinforced polymer reinforcement; GFRP: glass fiber–reinforced polymer.

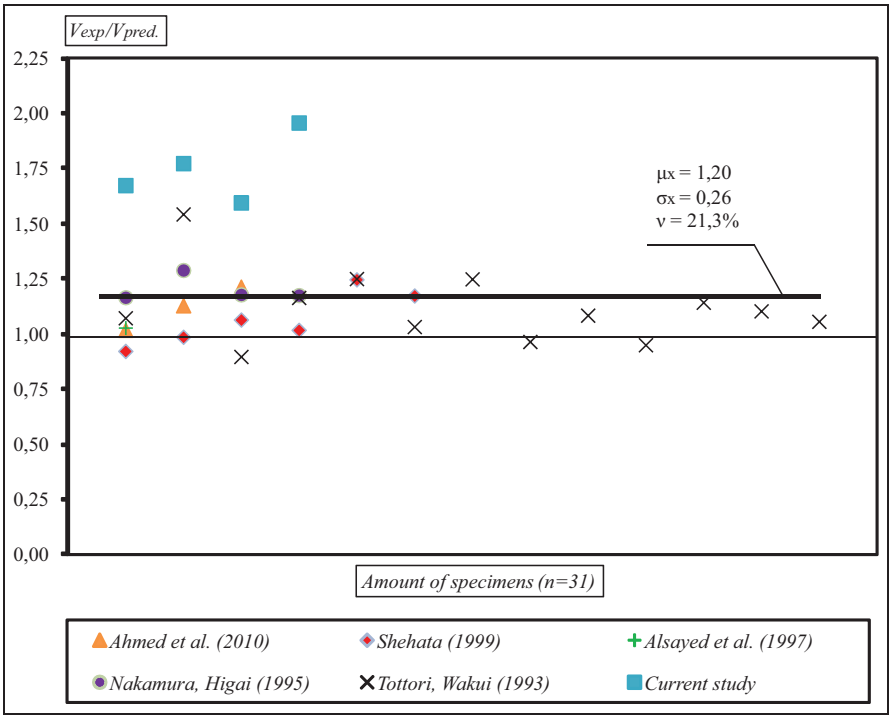

Figure 10. V_{exp}/V_{calc} values obtained by the proposed shear design model for beams reinforced with flexural steel and FRP shear reinforcement.

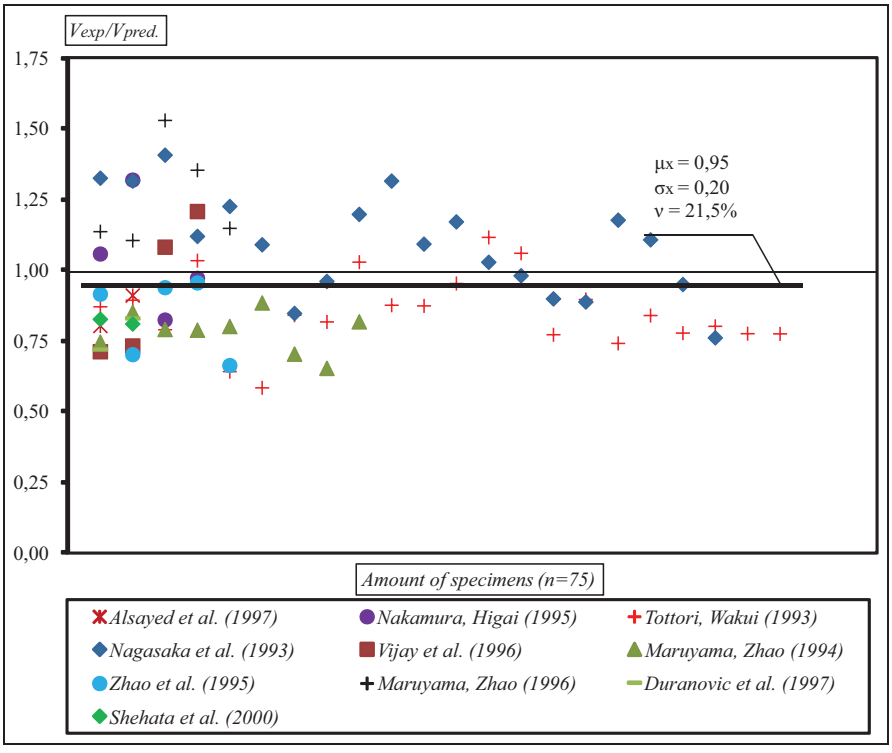

Figure 11. V_{exp}/V_{calc} values obtained by the proposed shear design model for beams reinforced with both flexural and shear FRP reinforcement.

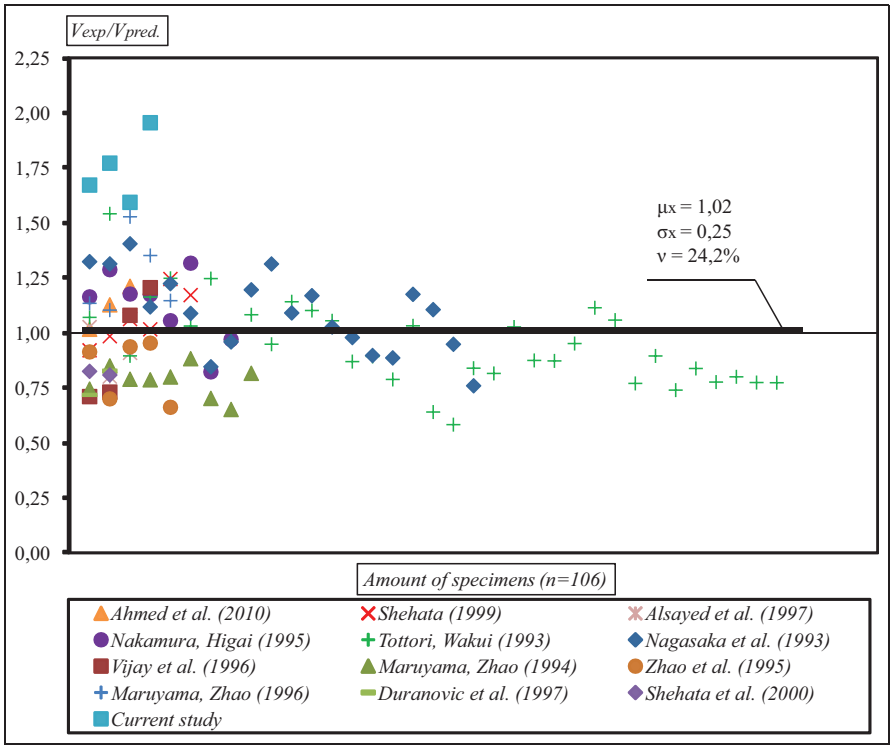

Figure 12. V_{exp}/V_{calc} values obtained by the proposed shear design model for beams reinforced with flexural steel or FRP reinforcement and FRP shear reinforcement.

Table 3. The comparison of experimental and calculated shear strength for beams reinforced with flexural steel or FRP reinforcement and with FRP stirrups.

Calculation model	Average V_{exp}/V_{calc}	Standard deviation σ_x	Coefficient of variation ν (%)
ACI 440.1R-06	1.29	0.49	37.8
JSCE	1.82	0.59	32.6
Eurocode 2	1.15	0.63	54.8
Sato et al.	1.07	0.33	30.7
Proposed shear design model	1.02	0.25	24.1

FRP: fiber-reinforced polymer; ACI: American Concrete Institute; JSCE: Japan Society of Civil Engineers.

in shear reinforcement is taken as 0.004 in EC 2 and ACI 440.1R-06 design recommendations, and the maximum strain is calculated using empirical equations as per JSCE, Sato et al. design recommendations and in the shear design model proposed by the authors of this article.

Table 3 gives the results of average V_{exp}/V_{calc} value, standard deviation, and coefficient of variation for all reviewed design recommendations and for proposed design model. The performance of the design equations was evaluated using the collected database for beams reinforced with flexural steel and FRP reinforcement and FRP shear reinforcement.

Table 3 shows that the most accurate method with the least scattered values is the proposed shear design model as the average V_{exp}/V_{calc} is 1.02 with a coefficient of variation of 24.1%.

Conclusion

This article has presented a comparative investigation regarding the shear resistance of FRP-reinforced concrete beams. The following conclusions can be drawn:

- The analysis of available shear strength calculation methods showed that there is no universal calculation model for calculating shear strength of concrete beams reinforced with FRP reinforcement. The available design recommendations are based on methods, which are intended for calculating shear resistance of steel-reinforced concrete beams. Therefore, these models do not properly take into account specific properties of FRP reinforcement. Design models have to be

modified using empirical equations, which could more accurately estimate the influence of the specific FRP properties.

- The results of the experimental tests of concrete beams reinforced with straight FRP shear stirrups showed that the anchorage is the main concern, when using non-metallic shear reinforcement. If straight FRP bars are used, they have to be securely fixed to the longitudinal reinforcement.
- Through comparative analysis of investigated design models, it was found that the most accurate model is the shear design model, proposed by the authors ($V_{exp}/V_{calc} = 1.02$, $\sigma_x = 0.25$, $\nu = 24.1\%$). The analytical values based on the proposed method are in good agreement with the experimental results. The suggested model is intended for calculating shear strength of concrete beams reinforced with FRP shear reinforcement. This model evaluates the influence of different types of FRP reinforcement for shear strength. The proposed equations allow to evaluate maximum strain of FRP shear reinforcement in order to control shear crack width.

Declaration of conflicting interests

The authors declare that there is no conflict of interests regarding the publication of this article.

Funding

This research received no specific grant from any funding agency in the public, commercial, or not-for-profit sectors.

References

1. Burgoyne C. Non-metallic reinforcement for concrete structures. In: *Proceedings of the international conference FRPRCS-5*, Cambridge, 16–18 July 2001. Thomas Telford Ltd.
2. Cosenza E, Manfredi G and Nanni A. Composites in construction: a reality. In: *Proceedings of the international workshop*, Capri, 20–21 July 2001, 277 pp. Reston, VA: ASCE.
3. Figueiras J, Juvandes L and Furia R. Composites in construction. In: *Proceedings of the CCC*, Porto, 10–12 October 2001. Balkema Publishers.
4. Japan Society of Civil Engineers (JSCE). *Recommendation for design and construction of concrete structures using continuous fiber reinforcing materials* (Concrete Engineering Series no.23). Tokyo, Japan: JSCE, 1997, 325 pp.
5. Teng JG. FRP composites in civil engineering. In: *Proceedings of the CICE*, Hong Kong, China, 12–15 December 2001. Elsevier Science.
6. Bashir R and Ashour A. Neural network modeling for shear strength of concrete members reinforced with FRP bars. *Compos B Eng* 2012; 43: 3198–3207.
7. Barris C, Torres L, Mias C, et al. Design of FRP reinforced concrete beams for serviceability requirements. *J Civ Eng Manag* 2012; 18: 843–857.
8. Fayyadh MM and Razak HA. Analytical and experimental study on repair effectiveness of CFRP sheets for RC beams. *J Civ Eng Manag* 2014; 20: 21–31.
9. Skuturna T and Valivonis J. The statistical evaluation of design methods of the load-carrying capacity of flexural reinforced concrete elements strengthened with FRP. *Arch Civ Mech Eng* 2015; 15: 214–222.
10. Daugevičius M, Valivonis J and Marčiukaitis G. Deflection analysis of reinforced concrete beams strengthened with carbon fibre reinforced polymer under long-term load action. *J Zhejiang Univ Sci A* 2012; 13: 571–583.
11. Sundarraja MC and Prabhu GG. Behaviour of CFST members under compression externally reinforced by CFRP composites. *J Civ Eng Manag* 2013; 19: 184–195.
12. Skuturna T and Valivonis J. Design method for calculating load-carrying capacity of reinforced concrete beams strengthened with external FRP. *Construct Build Mater* 2014; 50: 577–583.
13. Skuturna T, Valivonis J, Vainiūnas P, et al. Analysis of deflections of bridge girders strengthened by carbon fibre reinforcement. *Balt J Road Bridge E* 2008; 3: 145–151.
14. American Concrete Institute (ACI). *Guide for the design and construction of concrete reinforced with FRP bars*. ACI 440.1R-06, 2006, 44 pp., http://www.atp-frp.com/indice_ACI_440_1R_06.pdf
15. Canadian Standards Association (CSA). *Design and construction of building components with fiber reinforced polymers*. CAN/CSA S806-02, 2002, http://applications.roadauthority.com/Standards/?Id=61BE07D0-DD9B-4644-A7F5-5CD1668E7551
16. British Institution of Structural Engineers (BISE). *Interim guidance on the design of reinforced concrete structures using fiber composite reinforcement*. London: British Institution of Structural Engineers, 1999.
17. Advisory Committee on Technical Recommendations for Construction. *Guide for the design and construction of concrete structures reinforced with fiber-reinforced polymer bars*. CNR-DT 203/2006, 2007, http://www.cnr.it/documenti/norme/IstruzioniCNR_DT203_2006_eng.pdf
18. Currier J, Fogstad C, Walrath D, et al. Bond development of thermoplastic FRP shear reinforcement stirrups. In: *Proceedings of the third materials engineering conference*, San Diego, CA, 13–16 November 1994, pp.592–597. Reston, VA: ASCE.
19. Lees JM. Fibre-reinforced polymers in reinforced and prestressed concrete applications: moving forward. *Progr Struct Eng Mater* 2001; 3: 122–131.
20. Shehata E, Morphy R and Rizkalla S. Fibre reinforced polymer shear reinforcement for concrete members: behavior and design guidelines. *Can J Civil Eng* 2000; 27: 859–872.
21. Fico R, Prota A and Manfredi G. Assessment of Eurocode-like design equations for the shear capacity of FRP RC members. *Compos B Eng* 2008; 39: 792–806.
22. Machial R, Shahria Alam M and Rteil A. Revisiting the shear design equations for concrete beams reinforced with FRP rebar and stirrup. *Mater Struct* 2012; 45: 1593–1612.
23. Mari A, Bairan J, Cladera A, et al. Shear-flexural strength mechanical model for the design and assessment of reinforced concrete beams. *Struct Infrastruct E*. Epub

ahead of print 7 October 2014. DOI: 10.1080/15732479.2014.964735.
24. El-Sayed AK and Soudki K. Evaluation of shear design equations of concrete beams with FRP reinforcement. *J Compos Construct* 2011; 15: 9–20.
25. El-Sayed AK, El-Salakawy EF and Benmokrane B. Shear strength of concrete beams reinforced with FRP bars: design method. In: *Proceedings of the 7th international symposium on fiber-reinforced polymer (FRP) reinforcement for concrete structures (FRPRCS-7)*, Kansas City, MO, 6–9 November 2006, pp.955–974. American Concrete Institute.
26. Stratford T and Burgoyne C. Shear analysis of concrete with brittle reinforcement. *J Compos Construct* 2003; 7: 323–330.
27. Maruyama K and Zhao W. Flexural and shear behavior of concrete beams reinforced with FRP rods. In: Swamy RN (ed.) *Corrosion and corrosion protection of steel in concrete*. Sheffield: Sheffield Academic Press, 1994, pp.1330–1339.
28. Maruyama K and Zhao W. Size effect in shear behavior of FRP reinforced concrete beams. In: El-Badry M (ed.) *Advanced composite materials in bridges and structures*. Washington, DC: Transportation Research Board, 1996, pp.227–234.
29. Nagasaka T, Fukuyama H and Tanigaki M. Shear performance of concrete beams reinforced with FRP stirrups. In: *Proceedings of the international symposium on fibre reinforced-plastic reinforcement for concrete structures*, Vancouver, Canada, 28–31 March 1993, pp.789–811. American Concrete Institute.
30. Alsayed SH, Al-Salloum YA, Almusallam TH, et al. Evaluation of shear stresses in concrete beams reinforced by FRP bars. In: El-Badry M (ed.) *Advanced composite materials in bridges and structures*. Washington, DC: Transportation Research Board, 1996, pp.173–179.
31. Matthys S and Taerwe L. Concrete slabs reinforced with FRP grids. II: punching resistance. *J Compos Construct* 2000; 4: 154–161.
32. El-Ghandour AW, Pilakoutas K and Waldron P. Punching shear behavior of fiber reinforced polymers reinforced concrete flat slabs: experimental study. *J Compos Construct* 2003; 7: 258–265.
33. Ospina CE, Alexander SDB and Cheng JJR. Punching of two-way concrete slabs with fiber-reinforced polymer reinforcing bars or grids. *ACI Struct J* 2003; 100: 589–598.
34. Guadagnini M, Pilakoutas K and Waldron P. Shear performance of FRP reinforced concrete beams. *J Reinforc Plast Compos* 2003; 22: 1389–1408.
35. Guadagnini M, Pilakoutas K and Waldron P. Shear resistance of FRP RC beams: and experimental study. *J Compos Construct* 2006; 10: 464–473.
36. EN 1992-1-1:1992. Eurocode 2: design of concrete structures. Part 1-1: general rules and rules for buildings, 232 pp.
37. Sato Y, Ueda T and Kakuta Y. *Shear resisting model of reinforced and prestressed concrete beams based on finite element analysis*. Sapporo, Japan: Bulletin of the Faculty of Engineering, Hokkaido University, vol. 171, 1994.
38. Eshani MR, Saadatmanesh H and Tao S. Bond of hooked glass fiber reinforced plastic (GFRP) reinforcing bars to concrete. *ACI Mater J* 1995; 92: 391–400.
39. El-Sayed AK, El-Salakawy E and Benmokrane B. Mechanical and structural characterization of new carbon FRP stirrups for concrete members. *J Compos Construct* 2007; 11: 352–362.
40. Ahmed A, El-Salakawy EF and Benmokrane B. Shear performance of RC bridge girders reinforced with carbon FRP stirrups. *J Bridge Eng* 2010; 15: 44–54.
41. Shehata EFG. *Fiber reinforced polymer (FRP) for shear reinforcement in concrete structures*. PhD Thesis, Department of Civil and Geological Engineering, University of Manitoba, Winnipeg, MB, Canada, 1999.
42. Alsayed S, Al-Salloum Y and Almusallam T. Shear design of beams reinforced by GFRP bars. In: *Proceedings of the 3rd international symposium on non-metallic (FRP) reinforcement for concrete structures*, Sapporo, Japan, 14–16 October 1997, pp.285–292. Japan Concrete Institute.
43. Nakamura H and Higai T. *Evaluation of shear strength of concrete beams reinforced with FRP*, vol. 26. Tokyo, Japan: Concrete Library International (CLI), 1995, pp.111–123.
44. Tottori S and Wakui H. Shear capacity of RC and PC beams using FRP reinforcement. In: *Proceedings of the international symposium on fiber reinforced plastic reinforcement for concrete structures*, Vancouver, Canada, 28–31 March 1993, pp. 615–632. American Concrete Institute.
45. Nagasaka T, Fukuyama H and Tanigaki M. Shear performance of concrete beams reinforced with FRP stirrups. In: Nanni A and Dolan CW (eds) *Fiber-reinforced-plastic reinforcement for concrete structures—international symposium (SP-138)*. Vancouver, BC, Canada: American Concrete Institute, 1993, pp. 789–811.
46. Vijay PV and Kumar SV. Shear and ductility behavior of concrete beams reinforced with GFRP rebars. In: El-Badry M (ed.) *Advanced composite materials in bridges and structures*. Washington, DC: Transportation Research Board, 1996, pp.217–227.
47. Zhao W, Maruyama K and Suzuki H. Shear behavior of concrete beams reinforced by FRP rods as longitudinal and shear reinforcement. In: *Proceedings of the second international RILEM symposium on non-metallic (FRP) Reinforcement for Concrete Structures (FRPRCS-2)*, Ghent, 23–25 August 1995, pp. 352–359. E. & F. N. Spon.
48. Duranovic N, Pilakoutas K and Waldron P. Tests on concrete beams reinforced with glass fibre reinforced plastic bars. In: *Proceedings of the 3rd international symposium on non-metallic (FRP) Reinforcement for Concrete Structures (FRPRCS-3)*, Sapporo, Japan, 14–16 October 1997, vol. 2, pp.479–486. Japan Concrete Institute.

Appendix 1

Notation

a	shear span, mm
a_0	critical projection of shear cracking zone, mm

A_{fw} area of FRP shear reinforcement, mm^2
A_{fwi} area of one FRP reinforcement bar, mm^2
A_s area of steel reinforcement, mm^2
b_w width of the web, mm
c depth of compression zone at cracked transformed section, mm
d effective depth, mm
d_b diameter of the FRP bar in the bent portion, mm
E_f modulus of elasticity of longitudinal FRP reinforcement, MPa
$E_{flex.}$ modulus of elasticity of flexural reinforcement, MPa
E_{fw} modulus of elasticity of FRP shear reinforcement, MPa
E_s modulus of elasticity of longitudinal steel reinforcement, MPa
f_c compressive strength of concrete, MPa
f_{ct} tensile strength of concrete, MPa
f_{ctm} mean concrete tensile strength, MPa
f_{fb} tensile strength of FRP bent bar, MPa
f_{fuw} tensile strength of FRP shear reinforcement, MPa
f_{fw} stress level in the FRP shear reinforcement at the ultimate state, MPa
h height of the member, mm
k coefficient, which accounts the decreasing depth of neutral axis
L_{com} length of the horizontal zone, mm
L_f horizontal projection of the shear cracking zone, mm
L_{str} vertical projected length of the shear cracking zone, mm
n number of transverse reinforcement bars in the shear cracking zone
n_f modular ratio of modulus of elasticity of FRP reinforcement and concrete
r_b bending radius of FRP bar, mm
s spacing of shear reinforcement, mm
V_c concrete shear resistance, N
V_{calc} calculated shear strength, N
V_{com} shear resisting force by concrete at the horizontal zone, which connects compression and shear cracking zones, N
V_{exp} experimental shear strength, N
V_f FRP transverse reinforcement shear resistance, N
V_{str} shear resisting force by other than transverse reinforcement at the shear cracking zone, N
V_u shear capacity of FRP-reinforced concrete beam, N
$V_{u,f}$ value of shear force which can be resisted by the shear reinforcement, N
$V_{u,max}$ value of the maximum shear force which can be sustained by the member, limited by crushing of the compression struts, N
x_e depth of the compression zone, mm
z lever arm of internal forces, mm
α angle of the principal stress at the compression zone, °
α_{cw} coefficient taking into account the state of the stress in the compression chord
β angle of the principal stress at the horizontal zone, °
β_d coefficient, by which the size effect is estimated
β_n coefficient, which accounts the prestress of reinforcement
β_p coefficient, which accounts the specific properties of FRP reinforcement
$\bar{\varepsilon}_f$ average stirrup strain
ε_{fw} strain in the FRP stirrup at the ultimate state
$\varepsilon_{fw,lim}$ maximum strain in the FRP stirrup
θ angle between the concrete compression strut and the beam axis perpendicular to the shear force, °
ν coefficient of variation, %
ν_{fw} shear strength caused by web reinforcement in the structural member's linear meter, N/mm
ν_1 strength reduction factor for concrete cracked in shear
ρ_f longitudinal FRP reinforcement ratio
$\rho_{flex.}$ flexural reinforcement ratio
ρ_{fw} FRP shear reinforcement ratio
ρ_s longitudinal steel reinforcement ratio
$\bar{\sigma}_{com}$ average compressive stress at the horizontal zone, MPa
σ_{ct} concrete stress in the tensile zone, MPa
$\bar{\sigma}_f$ average tensile stress of web reinforcement at the shear cracking zone, MPa
σ_x standard deviation
$\bar{\tau}_c$ average shear stress at the compression zone, MPa
τ_m average shear stresses at the compression zone at loading point, MPa
$\bar{\tau}_{str}$ average shear stress at the shear cracking zone, MPa
φ_{c2}, φ_{c3},φ_{c4} coefficients which estimate concrete's properties
φ_f coefficient which estimates the specific flexural FRP reinforcement's properties